Capstone Project

Final Report

May 2018

Analysis into Conditional Corridor Variance Swap

Yuantao ZHANG[1]

Juncheng LI[2]

Weiyang WEN[3]

Xuan HUANG[4]

[1] yzhangfl@connect.ust.hk

[2] jlicv@connect.ust.hk

[3] wwen@connect.ust.hk

[4] xhuangbc@connect.ust.hk

Contents

List of Figures

1. Introduction

Variance swap is a forward contract on variance:

$$payoff = N \times (\sigma_{real}^2 - \sigma_K^2)$$

Conditional Corridor Variance Swap (abbreviated as CCVS) is a structure product facilitating risk recycling globally. This report mainly focuses on investigating various pricing approaches and their performances.

Compared with conventional volatility products, Conditional Corridor Variance Swap is innovated by separating corridor asset from the variance asset, as seen from its payoff structure:

$$\Pi_T = \frac{100}{2\mathbf{K}}\left[CorridorVar - \frac{1}{\mathbf{N}}\sum_{i=1}^{\boldsymbol{N}} w_i \mathbf{K^2}\right]$$

$$CorridorVar = \frac{\mathbf{252}}{\mathbf{N}}\sum_{i=1}^{\boldsymbol{N}} w_i \left(\ln\frac{S_1(t_i)}{S_1(t_{i-1})}\right)^2$$

$$w_i = 1_{\mathbf{L}<S_2(t_{i-1})<\mathbf{U}}$$

Where:

- N is the number of samples and is contractually agreed at inception.
- K is the strike of the swap
- L is the lower barrier of the corridor
- U is the upper barrier of the corridor
- wi measures whether the second asset is within the range $[L, U]$ at $ti-1$
- $S1$ is the variance asset
- S2 is the corridor asset

For simplicity, we safely assume that:

1. the currency of the payoff and both assets is the same.
2. the schedule is daily (daily close to close returns).
3. zero rate and dividend.

Some assumptions are relaxed depending on pricing method.

The pricing of such a payoff will depend critically on modelling asset 1's variance and Probability of asset 2 staying in the range, i.e., we need to back out corridor variance term, namely:

$$CorridorVar = \frac{\mathbf{252}}{\mathbf{N}}\sum_{i=1}^{\boldsymbol{N}} w_i \left(\ln\frac{S_1(t_i)}{S_1(t_{i-1})}\right)^2$$

$$w_i = 1_{\mathbf{L}<S_2(t_{i-1})<\mathbf{U}}$$

In further calculation, we decompose $w_i[L, U]$ into $w_i[0, U] - w_i[0, L]$, so that any corridor

is merely a strip of one sided corridor variance swaps. Focus on corridor variance can be justified by the property of swaps, where fix legs match the floating legs' expected value.

2. Stochastic Local Volatility Model

We define a model such that each asset follows dynamics below:

$$x_t^i = log\left(\frac{S_t^i}{S_0^i}\right)$$

$$dx_t^i = -\frac{1}{2}\sigma_{SLV}^i\left(t, x_t^i\right)^2 v_t dt + \sigma_{SLV}^i\left(t, x_t^i\right)\sqrt{v_t} dB_t^{x^i}$$

With:

$$v_t = \frac{1}{a_t} e^{u_t}$$

$$a_t = E(e^{u_t})$$

$$du_t = -\kappa u_t dt + \xi dB_t^u$$

For Stochastic Local Volatility Model, analytic solution is not applicable. The main goal of adapting Monte Carlo is to analyze the scale and trend of corridor variance against different parameters.

To simplify, we also assume that:

1. Once local volatility function $\sigma_{SLV}^i\left(t, x_t^i\right)$;
2. One vol of vol ξ, one κ for both models.

To achieve, we capture dynamics of both assets with local stochastic volatility model, where four Brownian Motion are needed. Therefore, we have six correlation parameters to investigate, formulating the correlation matrix below. Upper numeric notation 1,2 on the rho refers to variance asset and corridor asset respectively.

$$\begin{bmatrix} 1 & \rho^{x^1,x^2} & \rho^{x^1,u^1} & \rho^{x^1,u^2} \\ \rho^{x^1,x^2} & 1 & \rho^{x^2,u^1} & \rho^{x^2,u^2} \\ \rho^{x^1,u^1} & \rho^{x^2,u^1} & 1 & \rho^{u^1,u^2} \\ \rho^{x^1,u^2} & \rho^{x^2,u^2} & \rho^{u^1,u^2} & 1 \end{bmatrix}$$

2.1 Numerical Results for Stochastic Local Volatility Model

2.1.1 Sensitivity of Payoff against multiple correlation pairs

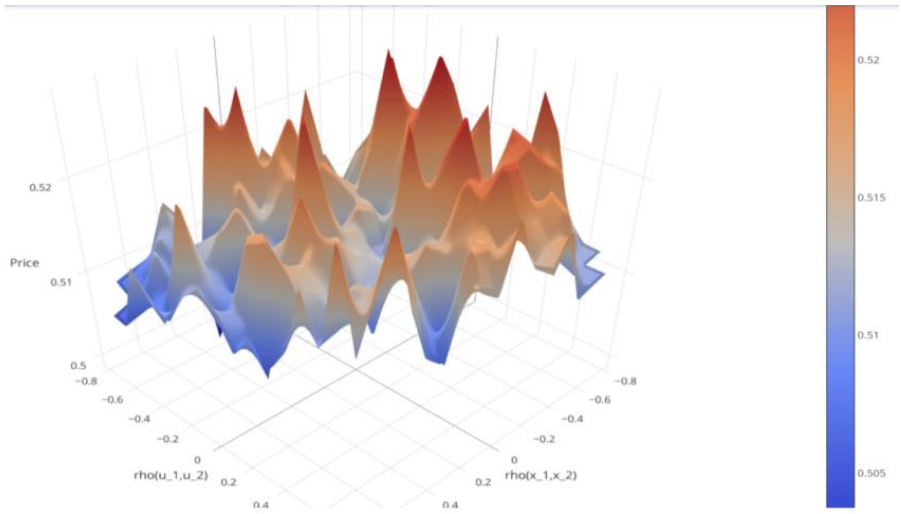

Figure 1 Payoff surface with changing ρ_{u_1,u_2} *and* ρ_{x_1,x_2}

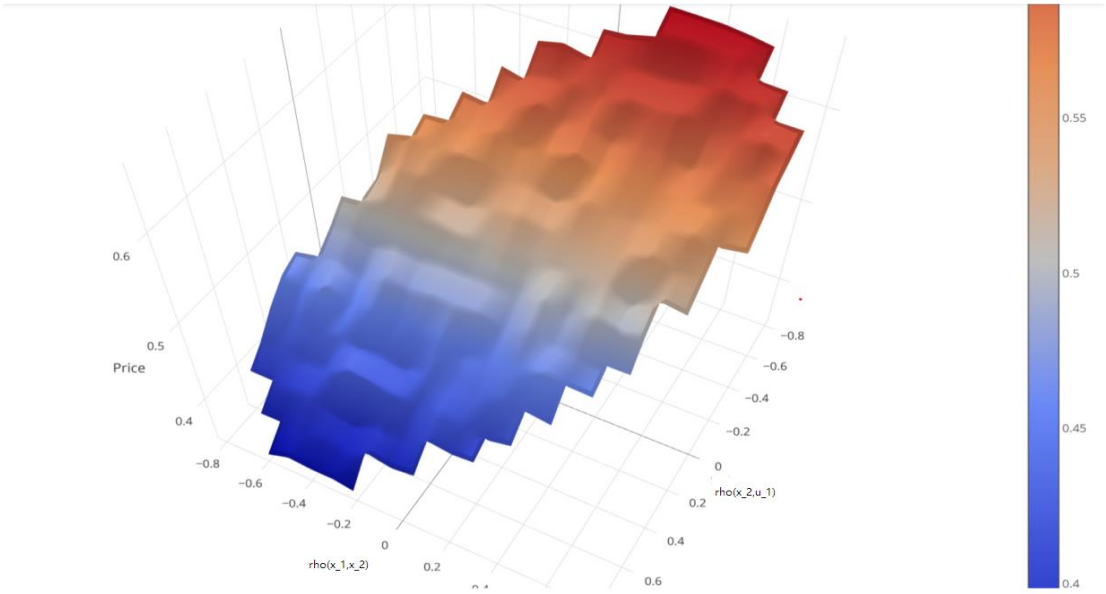

Figure 2 Payoff surface with changing ρ_{x_1,x_2} *and* ρ_{x_2,u_1}

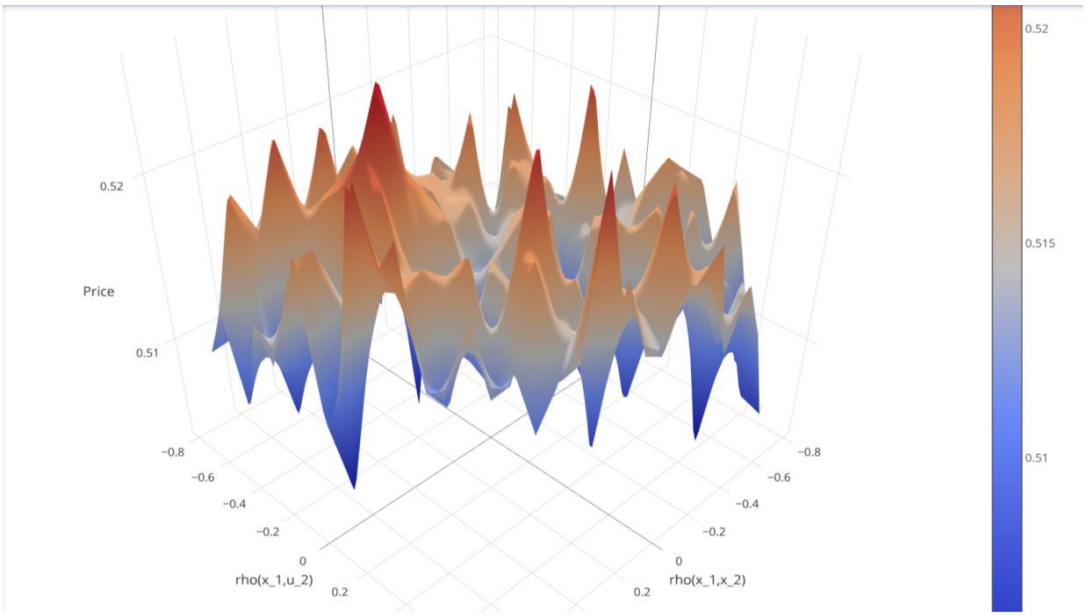

Figure 3 Payoff surface with changing ρ_{x_1,x_2} *and* ρ_{x_1,u_2}

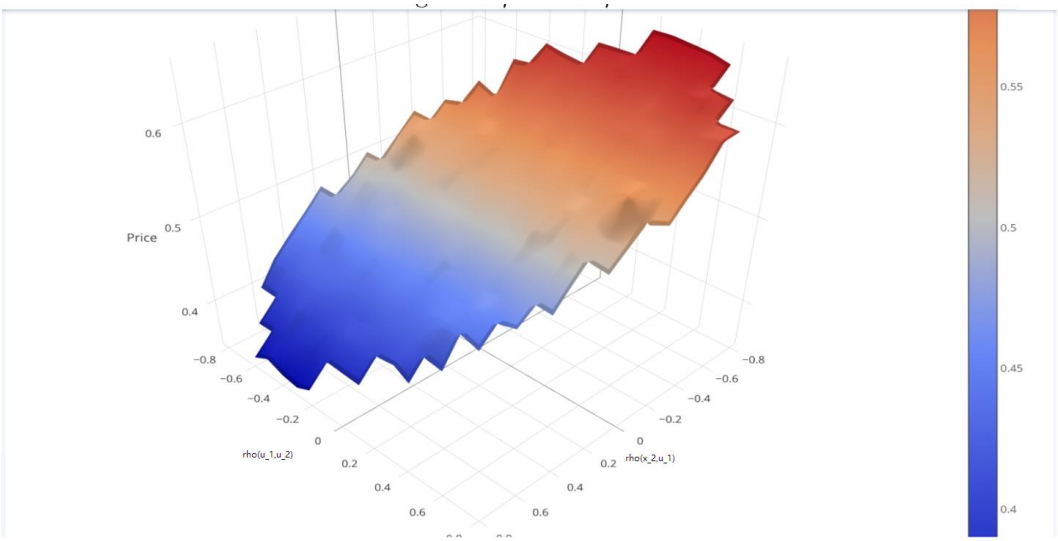

Figure 4 Payoff surface with changing ρ_{u_1,u_2} *and* ρ_{x_2,u_1}

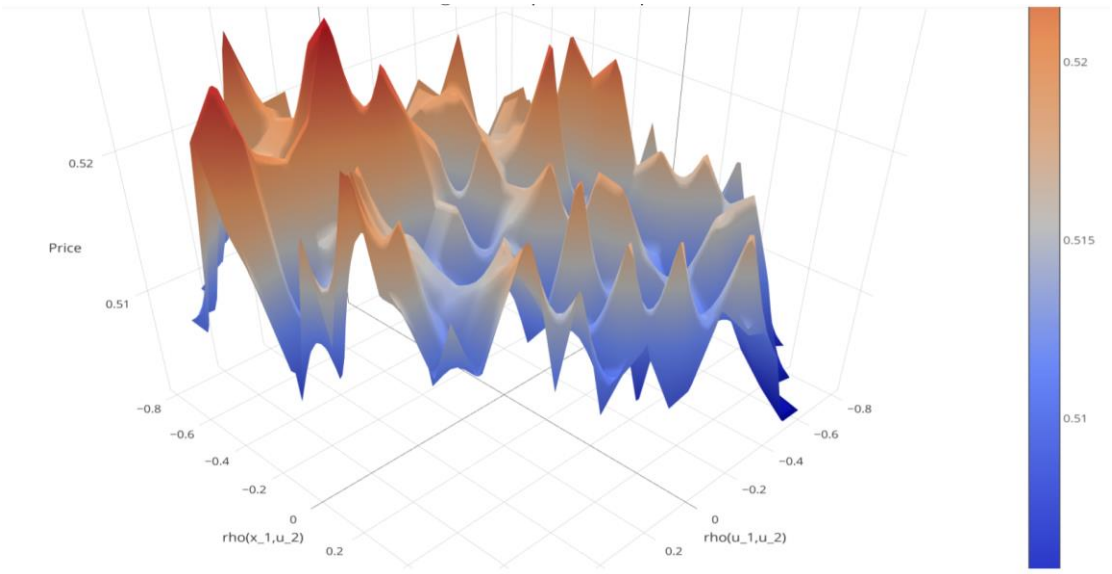

Figure 5 Payoff surface with changing ρ_{x_1,u_2} *and* ρ_{u_1,u_2}

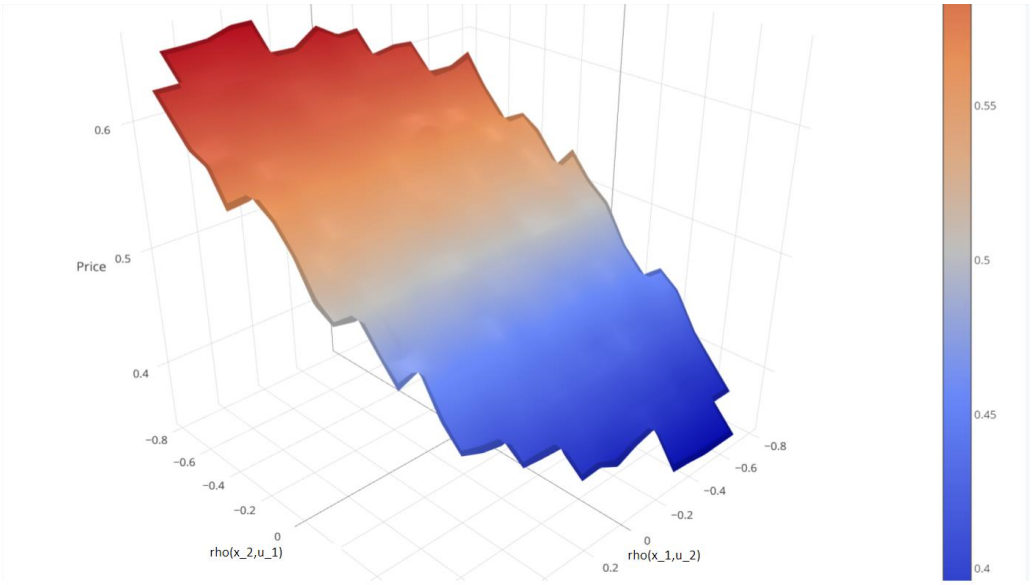

Figure 6 Payoff surface with changing ρ_{x_2,u_1} *and* ρ_{x_1,u_2}

2.1.2 Sensitivity of corridor variance against vol-spot correlation pair.

Throughout this section, we assumed time to maturity equal to 5 years.
The pricing of such payoff will depend critically on modelling the following factors:

1. Asset 1's variance;
2. Probability of asset 2 staying in the corridor;

Figure 7, Figure 8, Figure 9 and Figure 10 display the outcome.

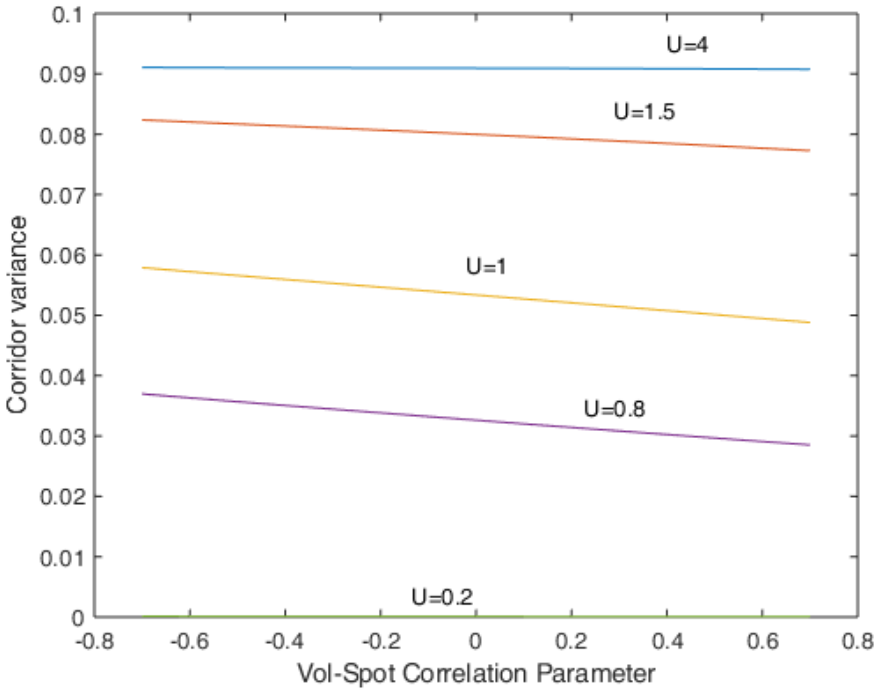

Figure 7 Estimated one-sided corridor variance with various U.

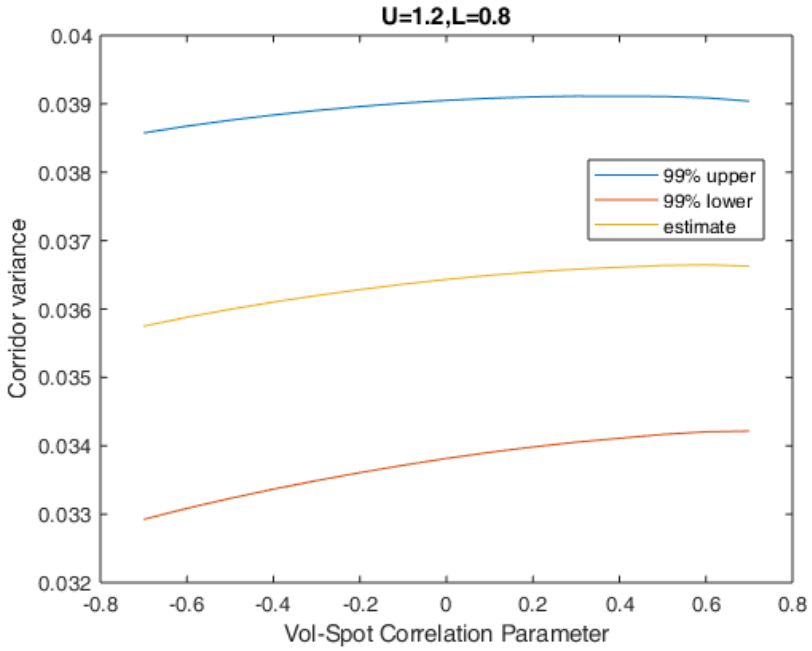

Figure 8 Estimated corridor variance with U=1.2, L=0.8, 99% confidence interval.

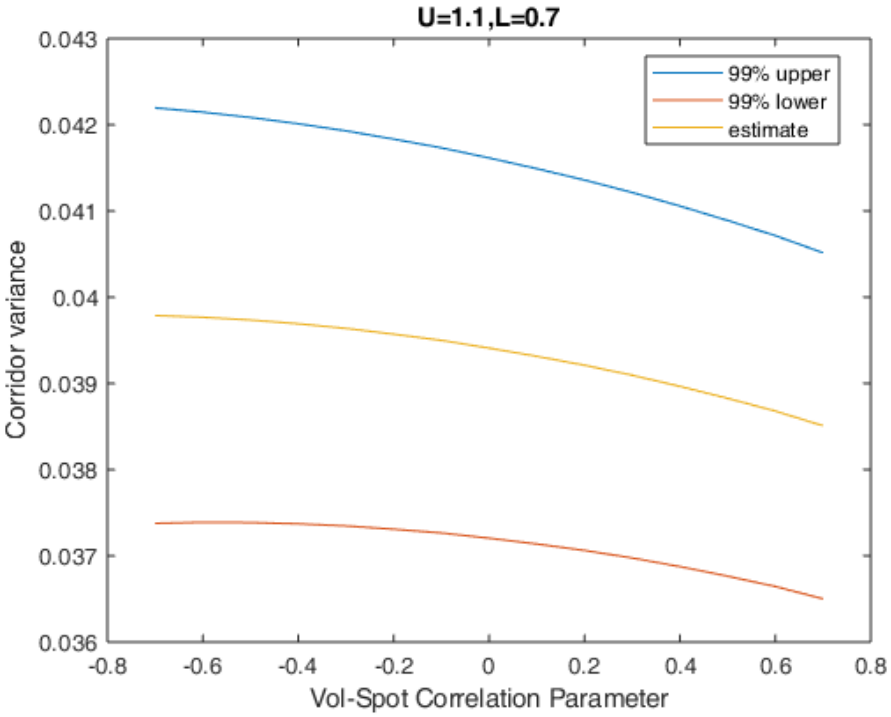

Figure 9 Estimated corridor variance with U=1.1, L=0.7, 99% confidence interval

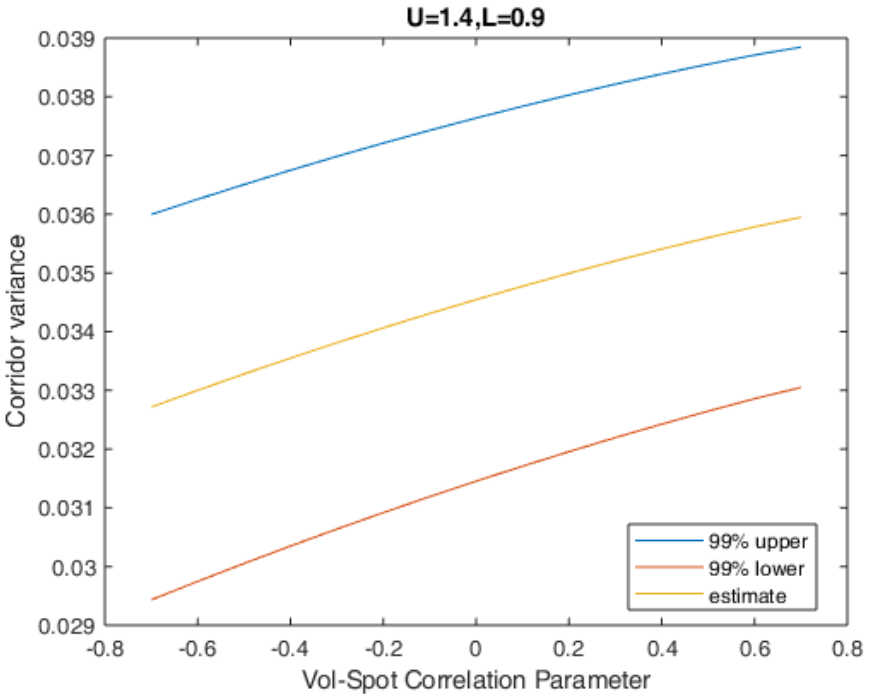

Figure 10 Estimated corridor variance with U=1.4, L=0.9, 99% confidence interval

2.2 Findings

1. Identified the risk driver[5] of CCVS.
    a. ρ^{u^1,x^2}. It can be justified with the payoff structure, affected by the variance and the corridor level simultaneously.
    b. ρ^{x^1,u^1}, ρ^{x^2,u^2} are not investigated since they are beyond the scope of our study.
    c. For the rest of correlation parameters, no contributions to the payoff except randomness, verified with numerical experiments.
2. Optimized test routines of the code:
    a. Formulated tabular input parameters. A handy tool for testing sensitivity of parameters and visualize outcomes.
    b. Optimized calculation routines mathematically.
        i. Screened out non-positive semi-definite correlation matrix before simulation.
    c. Investigated some variance reduction technique.
        i. Antithetic variables are unlikely to obtain desired improvement because the payoff structure depends on variance, not merely the log return.

2.3 Problems

Under daily simulation frequency, Calculation steps and required memory space for Monte Carlo grow linearly as maturity increases (e.g. up to 10 years). As a result, matrices storing computation results may occupy large proportion of memory available. With limited size of memory, computation time soars because system need to load matrices back and forth from the disk. The objective of following sections is to build simplified models with lower computational cost to consistently price this structure.

3. Common stochastic Volatility Model

This approach assumes that two spots S_t^1, S_t^2 share the same stochastic volatility process v_t. In this framework,

$$x_t^i = \log\left(\frac{S_t^i}{S_0^i}\right)$$

$$dx_t^i = -\frac{1}{2}\sigma_{SLV}^i\left(t, x_t^i\right)^2 v_t dt + \sigma_{SLV}^i\left(t, x_t^i\right)\sqrt{v_t} dB_t^{x^i}$$

With:

[5] To proceed Cholesky Factorization, Correlation Matrix must be positive definite. However, not all combination of parameters holds such property.

$$v_t = \frac{1}{a_t} e^{u_t}$$
$$a_t = E(e^{u_t})$$
$$du_t = -\kappa u_t dt + \xi dB_t^u$$

The model is proven to be failed. The model put too much restriction on solving the problem.

First, the original problem is to explore the correlation risk. Therefore, we should fix the marginal distribution while changing the correlations. This model poses a trouble that only ρ_{x^1,x^2} does not influence the marginal distribution of either asset. However, the main risk should come from the correlation between the vol of S_1 and the spot of S_2. To explore this correlation risk, we need to recalibrate each time we change ρ_{u,x^2}.

Second, the problem is hard to be solved under this model by any methods other than Monte Carlo. The origin document proposes an approach to price under this model. The problem is decomposed into two sub-problems:

1. solving a 2D elliptic PDE to find a corresponding European payoff so that the swap value can be replicated by a series of this kind of European contracts.
2. Pricing the corresponding European prices.

The corresponding elliptic PDE does not admit an analytical solution in general cases. If we solve the elliptic PDE by numerical methods such as finite element, we need to solve hundreds of PDE to get the necessary values for the European payoffs for the sub problem 2. Besides, the sub problem 2 should not be solved by numerical PDE since it is much more straightforward to solve the variance swap price directly.

We have proved the equivalence between solving the corresponding European and solving the original swap. This can be proven through the homogenization function in PDE theory.

We can write down the governing PDE of $\pi_t = E_t\left[\int_t^T \mathbf{1}_{L<S_2<U}\ {\sigma_1}^2 v_t dt\right]$ by

$$\frac{\partial \pi}{\partial t} - \kappa v(\ln v - \ln a_t)\frac{\partial \pi}{\partial v} + \frac{1}{2} v s_1^2 \sigma_1^2 \frac{\partial^2 \pi}{\partial s_1^2} + \frac{1}{2} v s_2^2 \sigma_2^2 \frac{\partial^2 \pi}{\partial s_2^2} + \frac{1}{2} v^2 \xi^2 \frac{\partial^2 \pi}{\partial v^2} +$$
$$\rho_{s_1,s_2} v s_1 s_2 \sigma_1 \sigma_2 \frac{\partial^2 \pi}{\partial s_1 \partial s_2} + \rho_{v,s_1} v^{\frac{3}{2}} s_1 \sigma_1 \xi \frac{\partial^2 \pi}{\partial v \partial s_1} + \rho_{v,s_2} v^{\frac{3}{2}} s_2 \sigma_2 \xi \frac{\partial^2 \pi}{\partial v \partial s_2} = -\mathbf{1}_{L<s_2<U} \sigma_1^2 v, \quad \text{(A)}$$

with the terminal condition $\pi(T, s_1, s_2, v) = 0$.

In original document, we let g(t; s1; s2) be the solution of following elliptic PDE. That is

$$\frac{1}{2} s_1^2 \sigma_1^2 \frac{\partial^2 g}{\partial s_1^2} + \frac{1}{2} s_2^2 \sigma_2^2 \frac{\partial^2 g}{\partial s_2^2} + \rho_{s_1,s_2} s_1 s_2 \sigma_1 \sigma_2 \frac{\partial^2 g}{\partial s_1 \partial s_2} = \mathbf{1}_{L<S_2<U} \sigma_1^2$$

For illustration purpose, we consider a simpler case where the local vol functions σ_i are state dependent only (i.e. $\sigma_i(t, s_i) = \sigma_i(s_i)$) We will see that $U_t = E_t\big(g(T;\ S1;\ S2)\big)$ is the solution of following terminal value problem:

$$\frac{\partial U}{\partial t} - \kappa v(\ln v - \ln a_t)\frac{\partial U}{\partial v} + \frac{1}{2}vs_1^2\sigma_1^2\frac{\partial^2 U}{\partial s_1^2} + \frac{1}{2}vs_2^2\sigma_2^2\frac{\partial^2 U}{\partial s_2^2} + \frac{1}{2}v^2\xi^2\frac{\partial^2 U}{\partial v^2} + \rho_{s_1,s_2}vs_1s_2\sigma_1\sigma_2\frac{\partial^2 U}{\partial s_1 \partial s_2} + \rho_{v,s_1}v^{\frac{3}{2}}s_1\sigma_1\xi\frac{\partial^2 U}{\partial v \partial s_1} + \rho_{v,s_2}v^{\frac{3}{2}}s_2\sigma_2\xi\frac{\partial^2 U}{\partial v \partial s_2} = 0 \quad \text{(B)}$$

with terminal condition $U(T; s_1; s_2; v) = g(T; s_1; s_2)$.

If we choose $g(t; s_1; s_2)$ as the homogenization function for terminal value problem (A), we will result in the terminal value problem (B). The solution is given by the following identities $U(t) = \pi(t) + g(t)$ and $\pi(0) = U(0) - g(0)$.

For the time dependent local vol σ_i, just applying Feynman-Kac on the term $E\left(\int_0^T \frac{\partial g}{\partial t}dt\right)$ and noticing that the terminal value is given by 0, we will derive the similar result.

4. Stochastic Variance and Local Corridor Model

4.1 Algorithm Build Up

In this model we mainly focus on the correlation between B.M. of variance asset's volatility process and B.M. of corridor assets' price. (Denoted as ρ throughout this section for notation simplicity) We assume that each asset follows the simplified diffusion:

$$\frac{dS_{1,t}}{S_{1,t}} = \sigma_{1,t}\sqrt{v_t}\,dW^1$$

$$\frac{dS_{2,t}}{S_{2,t}} = \sigma_2(t, S_{2,t})dW^2$$

With:

$$v_t = \frac{1}{\alpha_t}e^{u_t}$$

$$\alpha_t = \mathbb{E}[e^{u_t}] = \exp\left[\frac{\xi^2}{4\kappa}(1 - e^{-2\kappa t})\right]$$

$$du_t = -\kappa u_t dt + \xi dB_t^u$$

We can now focus on the computation of the term:

$$E\left(\sum_{i=1}^{N} 1_{L<S_2(t_{i-1})<U}\left(\ln\frac{S_1(t_i)}{S_1(t_{i-1})}\right)^2\right)$$

Under a daily schedule, the accumulated variance converges to the continuous variance case, i.e.:

$$\sum_{i=1}^{N} 1_{L<S_2(t_{i-1})<U}\left(\ln\frac{S_1(t_i)}{S_1(t_{i-1})}\right)^2 \xrightarrow{t_i-t_{i-1}\to 0} \int_0^T 1_{L<S_2(t)<U}\,\tilde{\sigma}^1_{SLV}\big(t,S_1(t)\big)^2 v_t dt$$

, where

$$\tilde{\sigma}^1_{SLV}\big(t,S_i(t)\big) = \sigma^i_{SLV}\big(t,x^i_t\big) = \sigma^i_{SLV}\left(t,\log\left(S^i_t/S^i_0\right)\right)$$

The pricing of the structure is then equivalent to the computation of the term:

$$E\Big(\int_0^T 1_{L<S_2(t)<U}\,\tilde{\sigma}^1_{SLV}\big(t,S_1(t)\big)^2 v_t dt\Big)$$

The key component of payoff is the evaluation of corridor variance (in a continuous limit sense):

$$\begin{aligned}
&\mathbb{E}\left[\int_0^T \sigma^2_{1,t}1_{L<S_{2,t}<U}\,v_t dt\right]\\
&=\int_0^T \sigma^2_{1,t}\left[\iint x\mathbb{1}_{L<y<U}\frac{\partial^2 F_t}{\partial x\,\partial y}(x,y)dxdy\right]dt\\
&=\int_0^T \sigma^2_{1,t}\left[\iint x\mathbb{1}_{L<y<U}C_{12}\big(F_{x,t}(x),F_{y,t}(y);\theta\big)f_{x,t}(x)f_{y,t}(y)dxdy\right]dt\\
&=\int_0^T \sigma^2_{1,t}\left[\iint_{[0,1]\times[0,1]} x\mathbb{1}_{L<y<U}C_{12}\big(F_{x,t}(x),F_{y,t}(y);\theta\big)\,dF_{x,t}(x)dF_{y,t}(y)\right]dt\\
&=\int_0^T \sigma^2_{1,t}\left[\iint_{[0,1]\times[0,1]} F^{-1}_{x,t}(u)\mathbb{1}_{F_{y,t}(L)<v<F_{y,t}(U)}\,C_{12}(u,v;\theta)dudv\right]dt\\
&=\int_0^T \sigma^2_{1,t}\left[\iint_{[-\infty,\infty]\times[0,1]} e^{\sqrt{2ln(a_t)}z-ln(a_t)}\mathbb{1}_{F_{y,t}(L)<v<F_{y,t}(U)}C_{12}(\Phi(z),v;\theta)\phi(z)\,dzdv\right]dt
\end{aligned}$$

where $\frac{\partial^2 F_t}{\partial x\,\partial y}$ is the copula density. Last line holds because $u_t \sim N\big(0,2ln(a_t)\big)$. This line is only for computational efficiency, since it is much faster to compute $\Phi(.)$ than $\Phi^{-1}(.)$. We will notice that the integral only depends on the marginal c.d.f of $S_{2,t}$ at corridor boundary. Therefore, we do not rely on the explicit form for marginal distribution. We assume the local vol of $S_{2,t}$is Dupire vol, which means we calibrate the marginal directly rather than a parameterized model. Actually, an extension of Derman and Kani (1998) gives the unique solution of $\sigma_2\big(t,S_{2,t}\big)$, that is:

$$\sigma_2(t,K)^2 = \sigma^2_{SLV,2}(t,ln\frac{K}{S_0})\mathbb{E}[v_{2,t}|S_T=K,S_0]$$

The dependence between $\Phi(z)$and $\Phi(v_t)$ can be captured with gaussian copula with predetermined correlation parameter. With proper transformations, we merely need to evaluate the expectation

$$E\left(T\sigma^2_{1,t}e^{\sqrt{2\ln(a_t)}z-\ln(a_t)}\mathbb{1}_{F_{y,t}(L)<v<F_{y,t}(U)}C_{12}(\Phi(z),v;\theta)\right)$$

Where $t\sim U(0,T), z\sim N(0,1), v\sim U(0,1)$.

This triple integral can be evaluated with Quasi Monte Carlo once we have obtained the

c.d.f. of corridor asset(S_2), and the realized variance of variance asset(S_1).

We also developed some code pieces to facilitate the application of Q.M.C. and copula.

$\sigma_{1,t}^2$ and $F_{S_2,t}(x)$ are treated as input parameters. Series of $\sigma_{1,t}^2$ are calibrated to variance swaps, and $F_{S_2,t}(x)$is calculated by pricing digital options $E[\mathbb{1}_{S_{2,t}<x}]$for various maturities and specific strikes. In our work, we chose L and U $\sim 0{,}0.1{,}0.2\cdots{,}3.9{,}4.0$. Data for calibration are generated from Local Stochastic Volatility Model by Monte Carlo approach.

In our calculation, we assume $\sigma_{SLV,1}(.) = 0.3$, a pure stochastic process S_1, and $dS_{2,t} = 0.3\sqrt{v_t}S_t^{\beta}dW_t$ with $S_{2,0} = 1$, a CEV type process to generate smile.

We priced all digital options with a same set simulation paths so that the calibration is very cheap. The above scheme works for any copulas if the copula density has a closed form, which is the case for most of usual copulas.

4.2 Numerical Results for Gaussian Copula

We calculated 5yrs CCVS floating leg with various corridors. We sampled 1 million points for computing the integral. Computational time is around 0.8s for each point and 1.5min for each correlation curve with CPU parallel computing.

The following figures show some examples of calculation results. For each figure in this section, x axis is the size of the correlation coefficient, y axis is the estimated size of corridor variance.

Figure 11 shows the integral value against ρ for various one-sided corridors under Gaussian Copula. Up corridor boundary value U are normalized by spot.

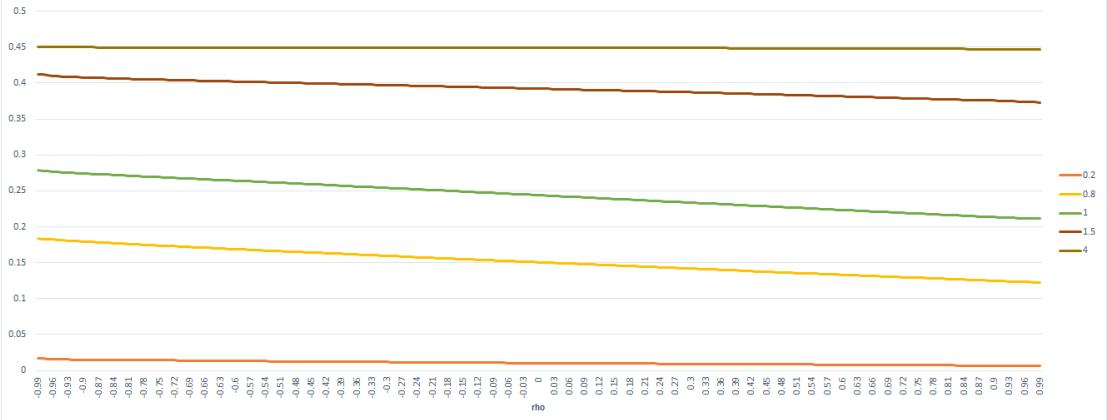

Figure 11 integral value with one sided corridor

The result is desirable. First, we can see that the integrated value is monotonically decreasing against ρ for all U. Second, when U goes to ∞ or 0, the curve becomes flat. Basing on this result, we expect to see different sensitivity for different corridor selections.

Figure 12, Figure 13 and Figure 14 show 3 distinct behavior due to different corridor selections. When U=1.2, L=0.8, the case for Figure 12,the curve is almost flat.

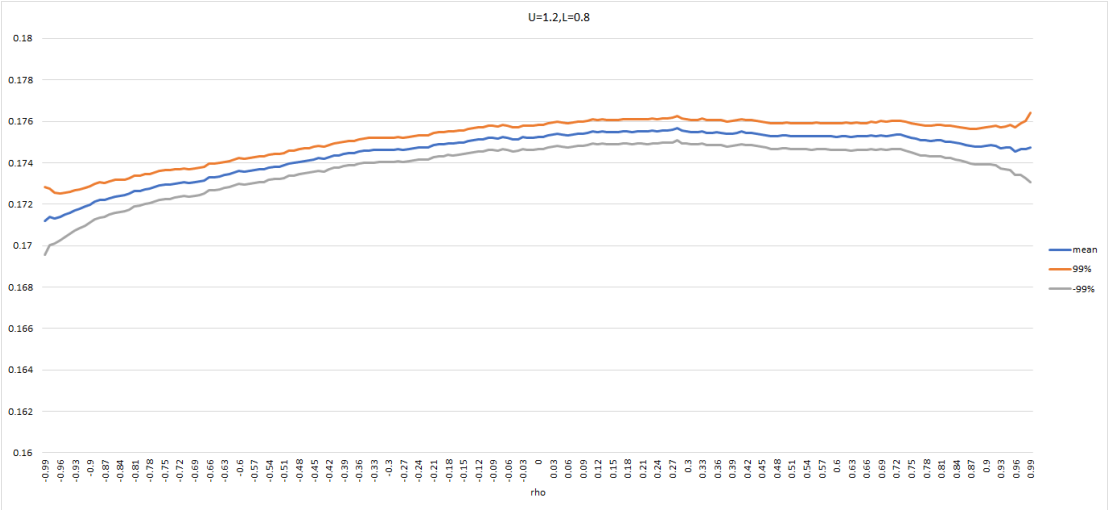

Figure 12 integral value for U=1.2, L=0.8 with 99% confidence interval

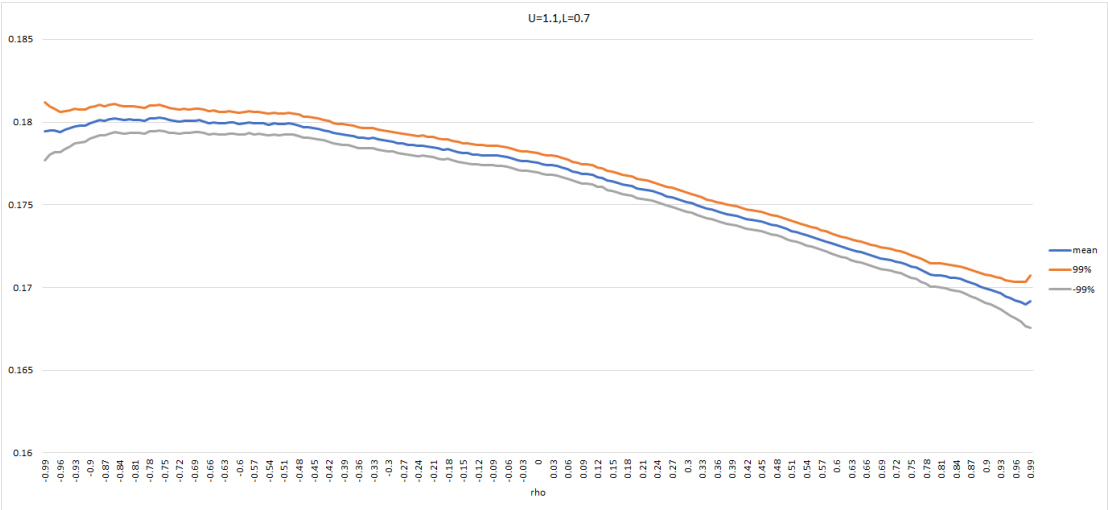

Figure 13 integral value for U=1.1, L=0.7 with 99% confidence interval

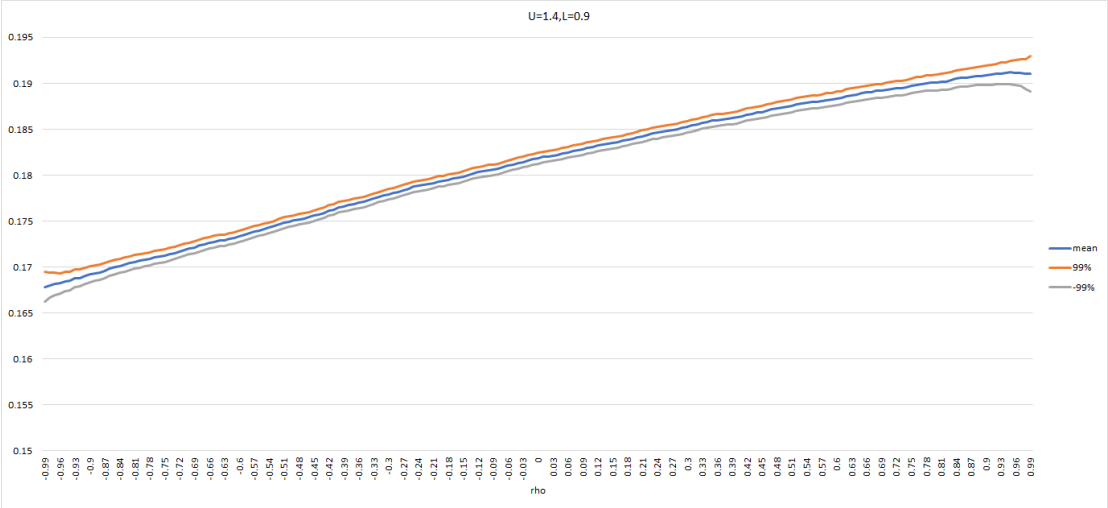

Figure 14 integral value for U=1.4, L=0.9 with 99% confidence interval

The numerical results regenerate the vol/spot correlation behavior in section 2. Corridor selection for Figure 13 is the same as that in section 2.

4.3 Other Copulas

We tried Farlie–Gumbel–Morgenstern (FGM) copula, defined as:

$$[C(u,v) = uv\big(1+\alpha(1-u)(1-v)\big), |\alpha| \le 1]$$

Figure 15 shows the calculation result under FGM copula with one-sided corridor.

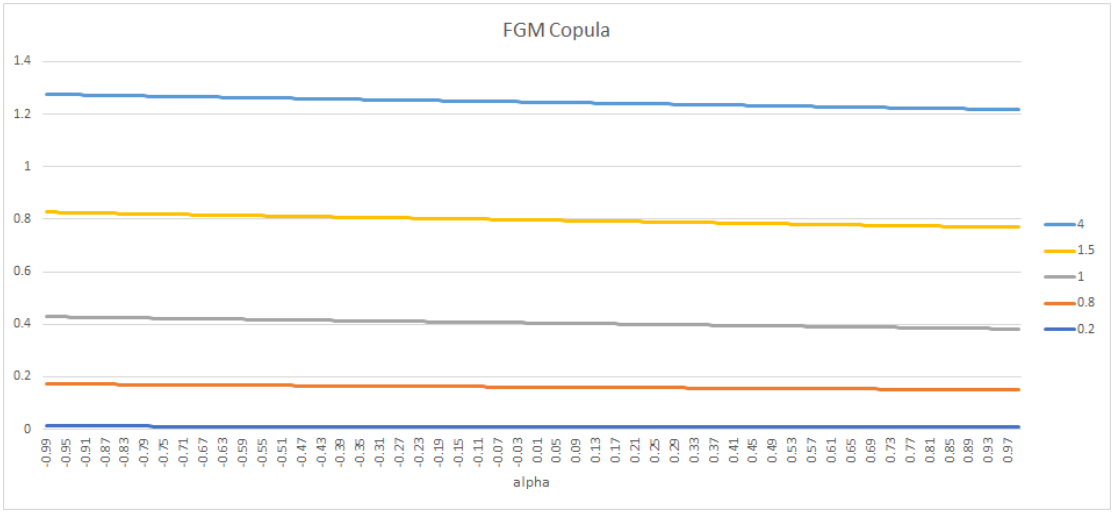

Figure 15 integral value with one sided corridor for FGM copula

We can see that the integral is still monotonically decreasing against copula parameter.\\
Figure 16, Figure 17 and Figure 18 show the numerical result under FGM copula with the

same parameters as those of Figure 12, Figure 13 and Figure 14.

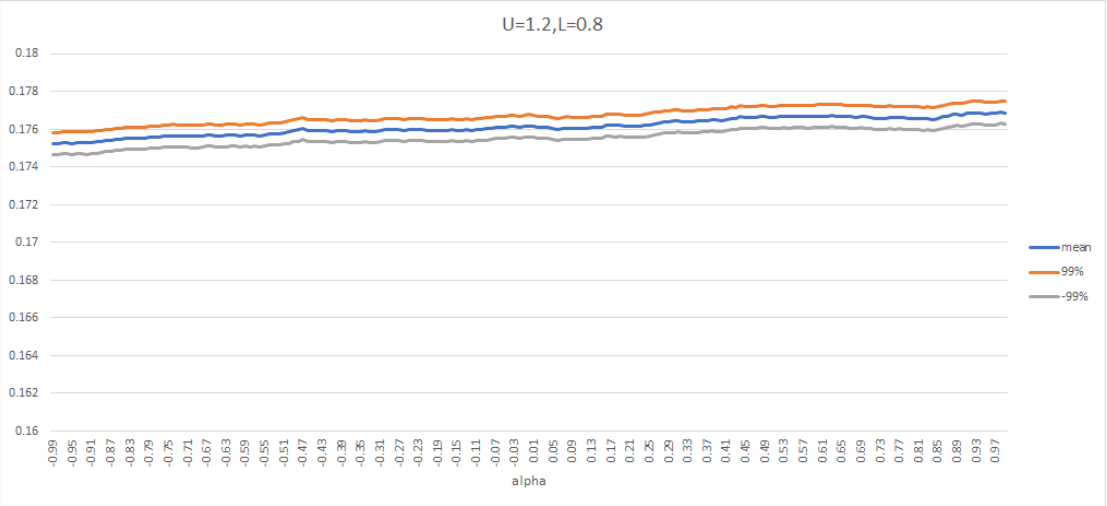

Figure 16 integral value for U=1.2, L=0.8 with 99% confidence interval

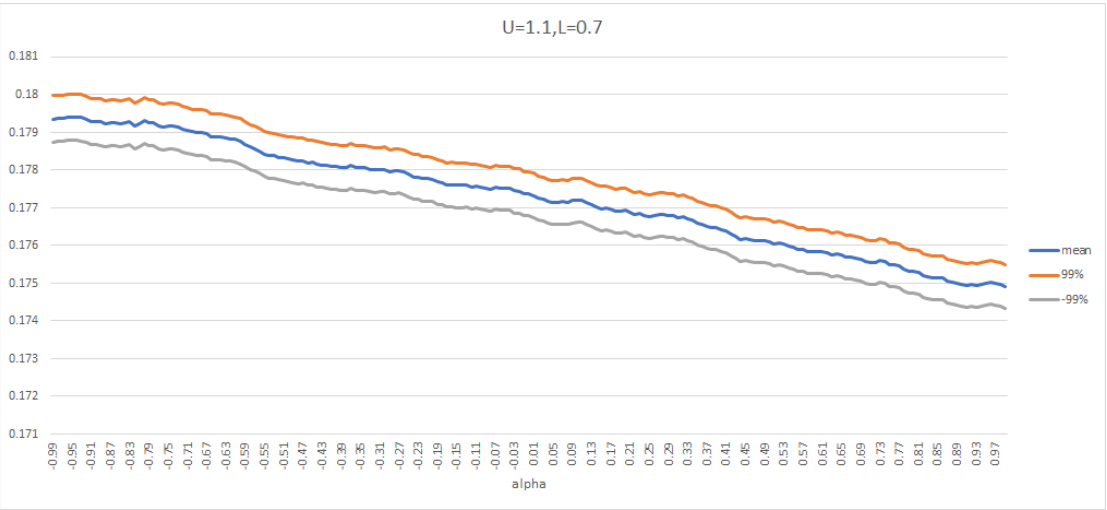

Figure 17 integral value for U=1.1, L=0.7 with 99% confidence interval

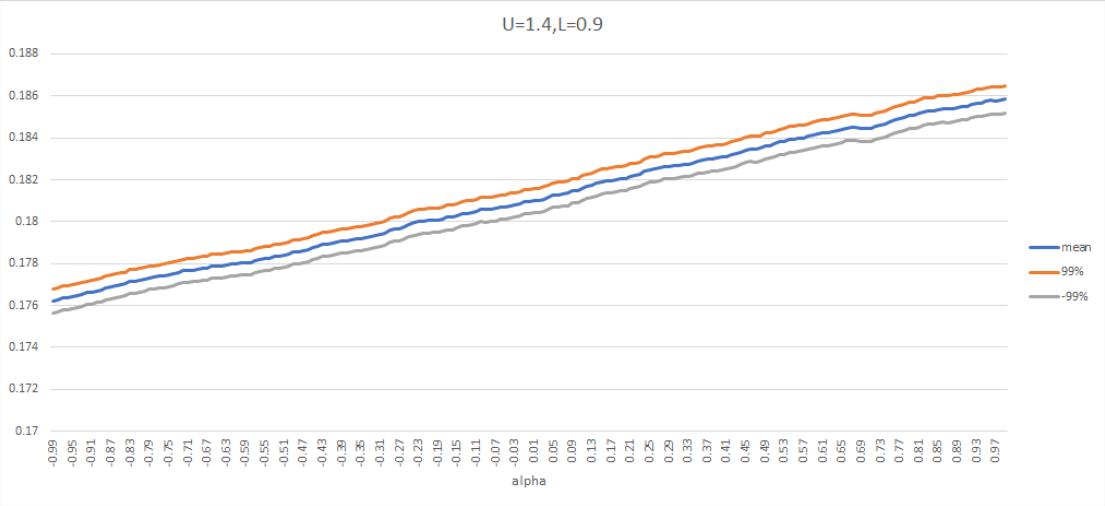

Figure 18 integral value for U=1.4, L=0.9 with 99% confidence interval

From results, we see that even though FGM copula gives different prices for one-sided corridor case, the two sided-corridor results resemble those of Gaussian copula.